Study on the interaction of anticancer drug mitoxantrone with DNA by fluorescence and Raman spectroscopies

Lingjuan Tang (汤玲娟), Zhenrong Sun (孙真荣), Jianyu Guo (郭建宇), and Zugeng Wang (王祖赓)

Key Laboratory of Optical and Magnetic Resonance Spectroscopy (East China Normal University), Ministry of Education, and Department of Physics, East China Normal University, Shanghai 200062,

Received August 10, 2005

Mitoxantrone, a clinically useful antitumour antibiotic for leukaemia and breast cancer, has received more attentions. In this paper, the interaction between mitoxantrone and calf thymus DNA is investigated by Raman and fluorescence spectroscopies, and the binding site of mitoxantrone to calf thymus DNA is explored. The results showed that mitoxantrone interacts with calf thymus DNA bases by the intercalation of anthracycline into the base pair plane of adenine (A) and thymine (T), and it results in the disruption of the hydrogen bonds between calf thymus DNA bases, and thus the calf thymus DNA double-strand can be disrupted into the B-form DNA double-strand segments.

OCIS codes: 170.5660, 170.0170, 000.1430, 300.6450.

It is important to understand the interaction of the anti-tumor and anti-viral drug and some carcinogenic molecules with DNA for designing new DNA-targeted drugs. Several techniques have been developed to study the interaction of DNA with drug molecules, including ultraviolet-visible spectroscopy, Raman spectroscopy, circular dichroism and electrochemical methods[1,2]. Raman spectrum, a non-destructive technique, can provide the detailed information about molecular structure and its chemical environment. Raman spectroscopy is often used to characterize the drug-DNA interaction and to monitor the effects of various drugs on DNA structure[3,4]. Moreover, it is all known that fluorescence spectroscopy is another useful technique for investigating DNA structure and dynamics[5,6].

The clinically useful anticancer drug mitoxantrone (1,4-dihydroxy-5,8-bis[[2-[(2-hydroxyethyl)amino]ethyl] amino]-9,10-anthracenedione) (MTX) is an aminoanthraquinone antibiotic. It has a planar heterocyclic ring structure (as shown in Fig. 1). It can intercalate into the base pairs of DNA by affinity, and result in the condensation and long-term DNA damage of nucleic acids. It is used to treat hepatoma, lymphocytic leukemia, breast carcinoma, non-Hodgkin's lymphomas and multiple sclerosis (MS)[7−9].

Recently, because it has stronger anti-tumor activity than that of adriamycin and less cardiotoxicity than other anthraquinone analogs, MTX has received more attention and the interaction of DNA with MTX has been especially investigated by a number of research groups.

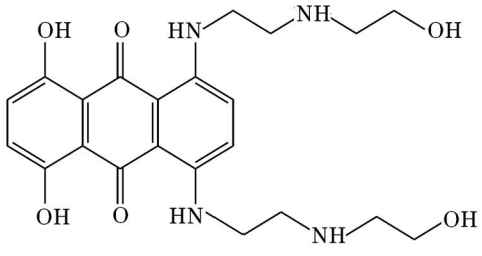

Fig. 1. Molecular structure of anticancer drug MTX.

The researches show that MTX interacts with DNA by the binding to its double helix[10,11], however the mechanisms for MTX to bind to the DNA double helix has not been completely understood. In this paper, we employ Raman and fluorescence spectroscopies to investigate the MTX-DNA complex and probe the drug binding site, and discuss the mechanism for the recognition process.

Calf thymus DNA and MTX were purchased from Sigma and used without further purification, and ethidium bromide (EB) was from Fluka. All other reagents were of analytical grade, and all of the solutions were prepared by triple-distilled water. The sample for Raman spectroscopy was prepared with pH7.0 phosphate buffer solution of 10^{-4} mol/L, and the MTX solution of 10^{-3} mol/L and the DNA solution of 30 mg/mL were mixed with the drug-to-DNA molar ratio of 1:10 and stirred for 24 hours. The samples for fluorescence measurement were obtained from the initial aqueous solution of MTX, DNA, and EB with the concentration of 10^{-2} mol/L, 1 mg/mL, and 10^{-5} mol/L, respectively. The initial solution was pH7.0 and contained 10^{-4} mol/L tris-HCl buffer and 50 mmol/L NaCl. The initial solutions of DNA and EB were mixed and stirred for 30 minutes, and then the initial solution of MTX was added and stirred for 30 minutes.

Raman spectra of DNA and DNA-MTX complex were recorded on a DILOR LabRan-1B Raman spectrophotometer at room temperature with the excitation wavelength of 632.8 nm and the power of 4 mW. Fluorescence spectra of DNA-EB and MTX complexes were obtained using a Hitachi F-4500 fluorescence spectrophotometer with the excitation wavelength of 525 nm and the emission wavelength of 595 nm.

Figure 2 shows Raman spectra of calf thymus DNA and DNA-MTX complex at room temperature with the excitation wavelength of 632.8 nm. The observed Raman frequencies of calf thymus DNA and DNA-MTX complex and their assignments are listed in Table 1. Generally, the band at 1094 cm^{-1} for PO_2^- symmetric stretching vibrational mode does not change for different DNA conformation, which is usually considered as an

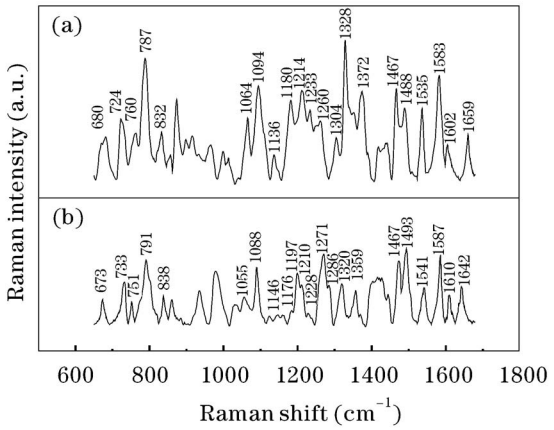

Fig. 2. Raman spectra for calf thymus DNA (a) and MTX-DNA complex (b).

Table 1. Raman Assignments of DNA and DNA-MTX Complex

DNA (cm^{-1})	DNA-MTX (cm^{-1})	Assignment[12−16]
680	673	G (δN7C8N9+δC5N7C8)
724	733	A (C2' Endo)
787	791	O–P–O Symmetric Stretch
832	838	O–P–O Asymmetric Stretch
1064	1055	C–O Stretch
1094	1088	PO_2^- Symmetric Stretch
1214	1210	G (δC8N9)
1233	1228	T (δC6H+C2N3)
1260	1271	C (δC6H+C4N4')
1304	1286	A (N9C8+N3C2+δC8H−δC2H)
1328	1320	T
1372	1359	A (Minor); T (Major)
1467	1467	Deoxyribose
1488	1493	A (δC2H+N9C8);
		G (δC8H−N9C8−C8N7)
1535	1541	G (Major); C (Minor)
1583	1587	G (C4N3+C5C4−N7C5);
		A (C5C4−C4N3)
1602	1610	A (δNH2−C5C6+C6N6');
		G (δNH2−C2N2');
		C (δNH2−C4N4')
1659	1642	T (C4=O−C5C4);
		C (C2=O−C2N3)

intensity standard. However, when calf thymus DNA interacts with MTX, the band for PO_2^- symmetric stretching vibrational mode shifts from 1094 cm^{-1} to 1088 cm^{-1} (as shown in Fig. 2 and Table 1), it indicates that partial DNA double-strand may be disrupted and the hydrogen bonds between the bases of DNA may be disrupted. The band at 787 cm^{-1} for the phosphor-diestreric O–P–O symmetric vibrational mode is sensitive to the DNA conformation. When MTX interacts with calf thymus DNA, the band shifts from 787 cm^{-1} to 791 cm^{-1}, and so it can be inferred that the double-strand of DNA is disrupted. Furthermore, the phosphor-diestreric O–P–O asymmetric stretching vibrational mode at 832 cm^{-1} is for the B form of calf thymus DNA. If the structure of DNA transforms from B to Z and A conformation, the phosphor-diestreric O–P–O asymmetric stretching vibrational mode will shift from 832 cm^{-1} for the B form to 810 cm^{-1} for the Z form and to 807 ± 3 cm^{-1} for the A form, respectively. As shown in Fig. 2 and Tables 1 and 2, the formation of the DNA-MTX complex leads to the shift of the phosphor-diestreric O–P–O asymmetric stretching vibrational band from 832 cm^{-1} to 838 cm^{-1}. It can be inferred that the shift is related to the disruption of the DNA double-strand, but there still exists the segment of the B form DNA double-strand[12−14].

As shown in Fig. 2 and Table 1, the band at 1602 cm^{-1} can be attributed to the dominant contributions from NH_2 — bending vibrational mode of the bases adenine (A), guanine (G) and cytosine (C), and the band at 1659 cm^{-1} to the contributions from the C=O stretching vibrational mode of the bases thymine (T) and cytosine (C)[15]. The intra-molecular hydrogen bonds can be formed between the C=O group of the base thymine or cytosine residues and the NH_2 group of the base adenine or guanine residues. If MTX intercalates into DNA, the hydrogen bonds will be disrupted, resulting in their Raman band shifts. As shown in Fig. 2 and Table 1, when MTX interacts with DNA, Raman bands at 1602 and 1659 cm^{-1} shift to 1610 and 1642 cm^{-1}, respectively. It indicates that the hydrogen bonds between the DNA bases are disrupted when MTX interacts with DNA.

Table 2. Relative Intensities of Raman Bands of DNA (I_{DNA}) and DNA-MTX Complexes ($I_{DNA-MTX}$) with Respect to the Raman Band at 1467 cm^{-1} for Deoxyribose. $\Delta = (I_{DNA} - I_{DNA-MTX})/I_{DNA} \times 100\%$

DNA (cm^{-1})	I_{DNA}	DNA-MTX (cm^{-1})	$I_{DNA-MTX}$	Δ (%)
680	0.76	673	0.68	10.5
724	1.4	633	1.1	21.4
787	2.2	791	1.81	18.2
832	1.1	838	0.8	27.2
1064	1.0	1055	0.8	20
1094	2.4	1088	1.4	41.6
1214	1.1	1210	0.94	14.5
1233	0.46	1228	0.32	30.4
1260	1.3	1271	1.2	7.7
1304	0.86	1286	0.62	27.9
1328	1.4	1320	1.1	21.4
1372	1.3	1359	0.92	29.2
1467	1.0	1467	1.0	0
1488	1.5	1493	1.2	20.0
1535	1.3	1541	1.2	7.7
1583	1.6	1587	1.4	12.5
1602	0.92	1610	0.74	19.6
1659	1.3	1642	1.2	7.7

The binding sites of the drug with DNA can be located by analyzing the Raman shifts and the relative intensities of DNA bases[16]. As shown in Fig. 2 and Tables 1 and 2, when MTX interacts with calf thymus DNA, the Raman bands for the stretching vibrations of adenine show more than 20% hypochromism and shift from 724, 1304, 1372, and 1488 cm^{-1} to 733, 1286, 1359, and 1493 cm^{-1}, respectively. The bands for the thymine show more than 15% hypochromism and shift from 1233 and 1328 cm^{-1} to 1228 and 1320 cm^{-1}, respectively. The Raman band at 1602 cm^{-1}, the major contribution from adenine, shows about 20% hypochromism. It is well-known that the drug molecule binding to the double helix of DNA can cause the hypochromism and be widely used as the evidence of stacked structures of various π-systems of nucleic acid bases[17−19]. As shown in Fig. 2 and Tables 1 and 2, the Raman bands with the contributions from adenine and thymine have considerable hypochromism of lager than 15%, and it indicates that the π-π electronic overlapping between π-electronic of anthracycline and π-electronic purine/pyrimidine rings of the bases of adenine and thymine, which can be induced by the intercalation of the MTX anthracycline chromophore into the DNA base pair plane of adenine and thymine, and the positively charged, nitrogen-containing side chains project out from the molecule and stabilize the ring in between base pairs by intercalating with the negatively charged phosphate backbone of DNA.

Therefore, the intercalation results in the permanent destruction of the DNA double-strand and the hydrogen bonds between their base pairs, and thus the calf thymus DNA double-strand is disrupted into the B form DNA double-strand segments.

In order to confirm the above hypothesis, the fluorescence spectroscopy is used to locate the MTX binding site in DNA by EB. EB is a phenanthridine fluorescence dye, it has weak fluorescence efficiency in the aqueous solution, however its fluorescence efficiency can be enhanced as it is bound to the DNA bases, and so it can usually be used as an excellent fluorescence probe for investigating the interaction between DNA and drug[20]. If a drug has the same binding site of DNA as EB, the drug as a rival will make EB away from the binding sites of DNA, and so it dramatically results in the decrease of the fluorescence intensity in the amalgam of DNA and EB as the drug added. If the fluorescence intensity of DNA-EB complex decreases down to about 50% as the concentration ratio of the drug to DNA-EB C_{drug}/C_{DNA} being 100, it can be indicated that the drug intercalates into DNA instead of EB with DNA[21,22]. Figure 3 shows the experimental curve for the fluorescence intensity as a function of the concentration ratio of MTX to DNA-EB. It shows that the fluorescence intensity decreases 73% when C_{drug}/C_{DNA} is 100, which means that MTX intercalates into the binding sites of DNA instead of EB.

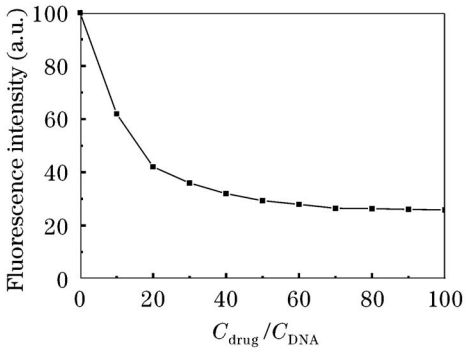

Fig. 3. Fluorescence intensity versus concentration ratio of MTX to DNA-EB.

In conclusion, the interaction of anticancer drug MTX with calf thymus DNA is studied by fluorescence and Raman spectroscopy. The results demonstrate the drug-DNA binding sites: MTX appears to bind to DNA by the anthracycline of MTX intercalating between the base pairs plane of adenine (A) and thymine (T). This interaction leads to the disruption of the hydrogen bonds between Calf thymus DNA bases, and thus the calf thymus DNA double-strand is disrupted into the B form DNA double-strand segments.

This work was supported by the National Natural Science Foundation of China (No. 10234030 and 10374030), the National Key Project for Basic Research of China (No. 1999075204), the Program for New Century Excellent Talents in University (NCET-04-0420), the Shanghai Science and Technology Committee (No. 036105019), and the Twilight Project sponsored by Shanghai Education Committee (No. 03SG23). Z. Sun is the author to whom the correspondence should be addressed, his e-mail address is zrsun@phy.ecnu.edu.cn.

References

1. D. W. Pang and H. D. Abruña, Analytical Chemistry **72,** 4700 (2000).
2. A. Erdem and M. Ozsoz, Analytica Chimica Acta **437,** 107 (2001).
3. H. Morjani, J. F. Riou, I. Nabiev, F. Lavelle, and M. Manfait, Cancer Research **53,** 4784 (1993).
4. J. M. Le Gal, H. Morjani, and M. Manfaint, Cancer Research **53,** 3681 (1993).
5. F. Seela and Y. Chen, Nucleic Acids Research **23,** 2499 (1995).
6. K. M. Guckian, T. R. Krugh, and E. T. Kool, Nature Structural Biology **5,** 954 (1998).
7. F. G. Loontiens, L. W. McLaughlin, S. Diekmann, and R. M. Clegg, Biochemistry **30,** 182 (1991).
8. J. A. Neidhart, D. Gochnour, and R. A. Roach, Journal of Clinical Oncology **4,** 672 (1986).
9. F. Brito-Babapulle, D. Catovsky, G. Slocombe, A. C. Newland, R. E. Marcus, J. M. Goldman, and D. A. Galton, Cancer Treatment Reports **71,** 161 (1987).
10. Y. A. Mao, W. Z. Wei, and S. F. Zhang, Anal. Bioanal. Chem. **373,** 215 (2002).
11. S. F. Wang, T. Z. Peng, and C. F. Yang, Biophys. Chem. **104,** 239 (2003).
12. H. Deng, V. A. Bloomfield, J. M. Benevides, and G. J. Thomas, Biopolymers **50,** 656 (1999).
13. E. Kocisova, L. Chinsky, and P. Miskovsky, Journal of Biomolecular Structure & Dynamics **15,** 1147 (1998).
14. T. Akira, H. Naoki, O. Junko, Y. Emiko, and T. Hideo, Journal of Raman Spectroscopy **30,** 623 (1999).
15. R. Dong, X. Yan, X. Pang, and S. Liu, Spectrochimica Acta Part A **60,** 557 (2004).
16. J. R. Chica, M. A. Medina, F. S. Jiménez, and F. J.

Ramìrez, Biochimica et Biophysica Acta **1628,** 11 (2003).
17. P. Yang, M. L. Guo, and B. S. Yang, Chin. Sci. Bulletin (in Chinese) **38,** 2049 (1993).
18. Q. S. Li, P. Yang, H. F. Wang, and M. L. Guo, Journal of Inorganic Biochemistry **64,** 181 (1996).
19. V. E. Semenov, V. D. Akamsin, V. S. Reznik, A. V. Chernova, G. M. Dorozhkina, Y. Y. Efremov, and A. A. Nafikova, Tetrahedron Lett. **43,** 9683 (2002).
20. W. J. Jin, Y. S. Wei, C. S. Liu, G. L. Shen, and R. Q. Yu, Spectrochimica Acta Part A **53,** 2701 (1997).
21. C.-W. Ong, Inorganica Chimica Acta **123,** 221 (1986).
22. Y. Ye, J. M. Hu, and Y. Zeng, Inorganica Chimica Acta **16,** 6 (2000).